

ELECTROMAGNETIC INTERFERENCE PREDICTION OF  
A FLYBACK SWITCHMODE POWER SUPPLY USING  
SIMULATION TECHNIQUES

T. P. Robbins

TELECOM RESEARCH LABORATORIES  
770 BLACKBURN ROAD, CLAYTON, VICTORIA 3168  
AUSTRALIA

ABSTRACT

Switchmode power conversion is displacing conventional linear power conversion within Telecom Australia exchange equipment. The increasing use of switchmode power conversion has brought advantages through reduced size and weight and higher efficiency. However when such equipment is poorly designed and/or constructed then considerable levels of electromagnetic interference are generated, and problems are caused both within the network and to other electronic equipment nearby.

Advances in computer aided design software and device models have enabled the waveforms within a switchmode power supply to be accurately simulated. As a result of this, simulation techniques can be used to predict conducted interference levels generated by a switchmode supply and to design circuit solutions.

INTRODUCTION

Switchmode power conversion is being introduced into the exchange environment, and is used in dc-to-dc distribution of 48V dc power, battery chargers (rectifiers), inverters and uninterruptible power supplies (UPS), with power ratings up to 10kW. A growing range of customer premises equipment (CPE) for ISDN will also use switchmode power conversion. The advantages of switchmode power supplies for Telecom Australia are in the size and weight reduction of installed and transportable electrical equipment and its higher efficiency.

However, the increasing use of switchmode power conversion has led to an awareness of the interference generated by the switchmode process. In the past, too often power supply engineers have focussed on efficiency increase in their circuit development, including interference suppression as an addendum. This situation has led to interference from switchmode power supplies causing many communication problems. These have been addressed by Telecom Australia, resulting in the design of retrofit kits and their 'as required' application to date. This paper reports on the development of simulation techniques to model the operation of switchmode supplies and to predict conducted interference levels.

Computer aided assessment of switchmode power supplies has been reported using state-space averaging techniques<sup>1</sup> which transform the switching circuit into an equivalent circuit without switching.

However to assess switching losses and interference spectra requires accurate simulation waveforms of the circuits voltages and currents during switching transitions. This level of simulation accuracy requires suitable transient (high-frequency) models of semiconductor and passive components within switching circuits.

Readily available low-frequency device models can be developed into accurate high-frequency models, and this paper describes such a model for the power Mosfet. Initial modelling procedures for power Mosfet devices operating in squarewave converters<sup>2,3</sup> have obtained poor correlation between experimental and simulated switching waveforms, with 2:1 discrepancies in transition times. A model for the power Mosfet device has been developed which achieves good correlation between simulated and measured switching waveforms when operating in a square-wave converter. The critical area for modelling the Mosfet device was the non-linear voltage-dependent drain-gate capacitance.

Once suitable component models have been developed, conventional analogue simulation software can be used to generate voltage and current waveforms occurring in the converter circuit. A Fast Fourier Transform is then used on the specified time-domain waveform to obtain the resulting frequency spectrum.

A model has been developed of an offending flyback switchmode power supply to obtain interference frequency spectra using simulation techniques. The power supply under investigation was situated within a PABX and was causing interference in customer premises. Good correlation has been achieved between simulated and measured time-domain switching waveforms when values for the circuit components and dominant parasitics are accurately represented.

Measurements were taken in the Telecom Australia Research Laboratories of levels of mains borne EMI from a commonly-available PABX, and found that they did not comply with the EMI limits specified by the International Special Committee on Radio Interference (CISPR) in CISPR Publication 22<sup>4</sup> and by the United States Federal Communications Commission (FCC) in the Code of Federal Regulations<sup>5</sup>. Frequency spectra from the EMI measurements are compared with simulated spectra from the power supply model.

conducted to date show a divergence in operating conditions with successive switching periods.

A suitable Mosfet model is therefore still to be developed. A simple solution can be found by redefining the capacitance equation for the SPICE pn diode model so that the junction capacitance is a constant for negative  $V_{dg}$ . This would allow the two-capacitor network model from Xu and Schroder to be reduced to one component, alleviating any voltage sharing problems. However, the ability to change software code for the diode model is not an option in general.

The capacitor model developed to define  $C_{dg}$  in this paper is a switched three-capacitor network, as shown in Figure 2. Capacitance  $CDG1$  defines  $C_{dg}$  for  $V_{dg} > +10V$ , and uses the constant drain-gate capacitance in the SPICE Mosfet model. A voltage dependent capacitance  $CDG2$  is used to define  $C_{dg}$  for  $V_{dg}$  between  $-2V$  and  $+10V$ , and is described by a second-order power series expression. A constant capacitor  $CDG3$  is used to define  $C_{dg}$  for  $V_{dg} < -2V$ . The value of  $CDG2$  at  $+10V$  is equated with  $CDG1$ , and at  $-2V$  is equated with  $CDG3 + CDG1$ .

The voltage controlled switches are used to connect  $CDG2$  and  $CDG3$  into the circuit during the appropriate range of  $V_{dg}$ . The switch is not a standard SPICE component, but is available in the simulation software PSpice used for this paper. The switch is a voltage controlled resistor, with a value varying from 1megohm in the off-state to 1ohm in the on-state. The control voltage range is made broad (2-3V) to alleviate potential computational problems caused by the gain of the switch. The value of  $C_{dg}$  during the switch voltage transitions ( $-2V$  and  $+10V$ ) can be controlled to give a smooth or peaked change in capacitance, as specified by the transition characteristics of the switches.

The performance of the  $C_{dg}$  model for an IRF130 Mosfet type was tested by ramping a voltage across the capacitance linearly from  $-10V$  to  $+25V$ , and back to  $-10V$ , at a rate of 35V/usec. The simulated capacitance variation with voltage is shown in Figure 3 along with the measured curve from Figure 1. A smooth capacitance transition is achieved at  $+10V$  and a peaked capacitance response occurs at  $-2V$  as required.

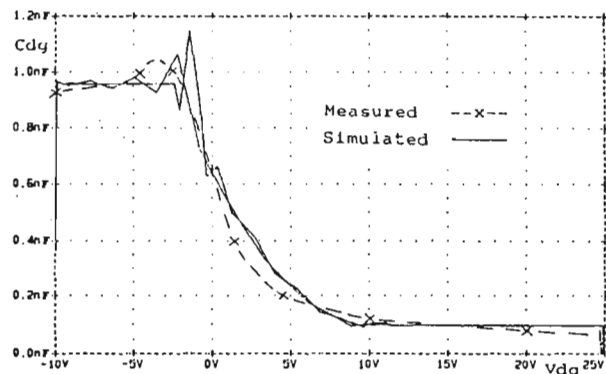


Figure 3. Simulated and measured variation of  $C_{dg}$  versus  $V_{dg}$  for IRF130 Mosfet.

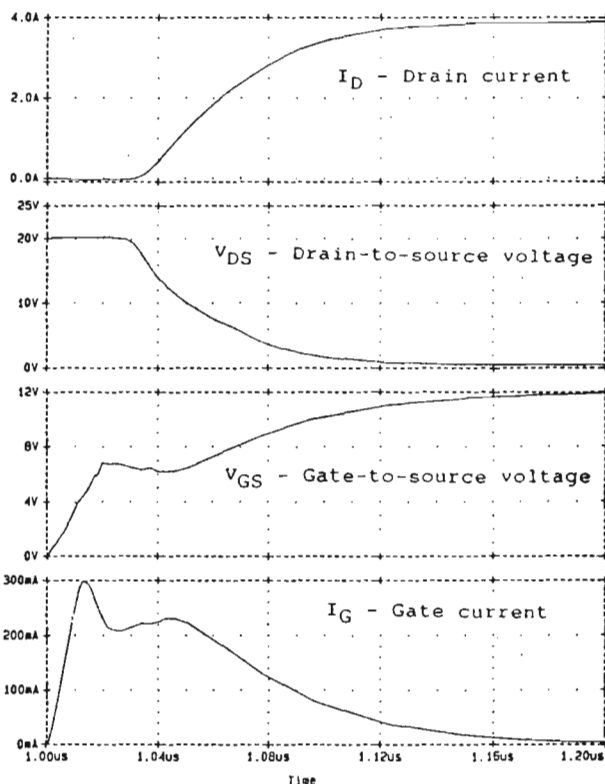
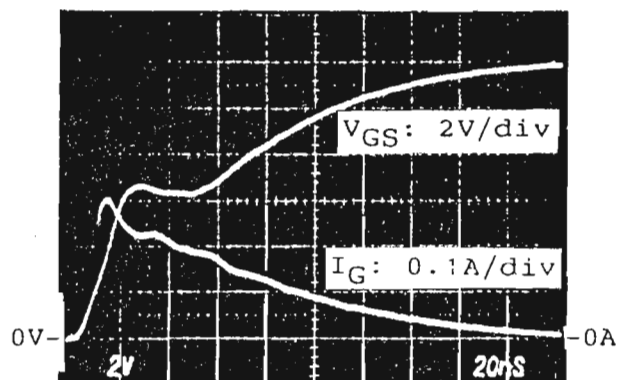
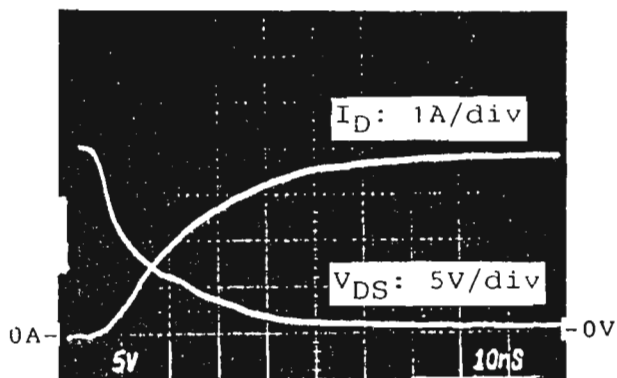


Figure 4a. Measured<sup>8</sup> and simulated Mosfet switching waveforms during turn-on in a resistive load circuit.

conducted to date show a divergence in operating conditions with successive switching periods.

A suitable Mosfet model is therefore still to be developed. A simple solution can be found by redefining the capacitance equation for the SPICE pn diode model so that the junction capacitance is a constant for negative Vdg. This would allow the two-capacitor network model from Xu and Schroder to be reduced to one component, alleviating any voltage sharing problems. However, the ability to change software code for the diode model is not an option in general.

The capacitor model developed to define Cdg in this paper is a switched three-capacitor network, as shown in Figure 2. Capacitance CDG1 defines Cdg for Vdg > +10V, and uses the constant drain-gate capacitance in the SPICE Mosfet model. A voltage dependent capacitance CDG2 is used to define Cdg for Vdg between -2V and +10V, and is described by a second-order power series expression. A constant capacitor CDG3 is used to define Cdg for Vdg < -2V. The value of CDG2 at +10V is equated with CDG1, and at -2V is equated with CDG3+CDG1.

The voltage controlled switches are used to connect CDG2 and CDG3 into the circuit during the appropriate range of Vdg. The switch is not a standard SPICE component, but is available in the simulation software PSpice used for this paper. The switch is a voltage controlled resistor, with a value varying from 1megohm in the off-state to 1ohm in the on-state. The control voltage range is made broad (2-3V) to alleviate potential computational problems caused by the gain of the switch. The value of Cdg during the switch voltage transitions (-2V and +10V) can be controlled to give a smooth or peaked change in capacitance, as specified by the transition characteristics of the switches.

The performance of the Cdg model for an IRF130 Mosfet type was tested by ramping a voltage across the capacitance linearly from -10V to +25V, and back to -10V, at a rate of 35V/usec. The simulated capacitance variation with voltage is shown in Figure 3 along with the measured curve from Figure 1. A smooth capacitance transition is achieved at +10V and a peaked capacitance response occurs at -2V as required.

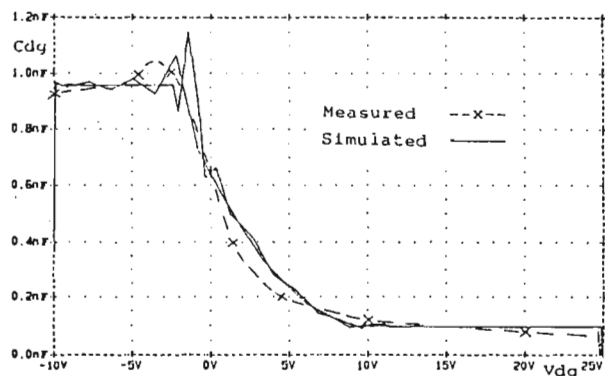


Figure 3. Simulated and mesured variation of Cdg versus Vdg for IRF130 Mosfet.

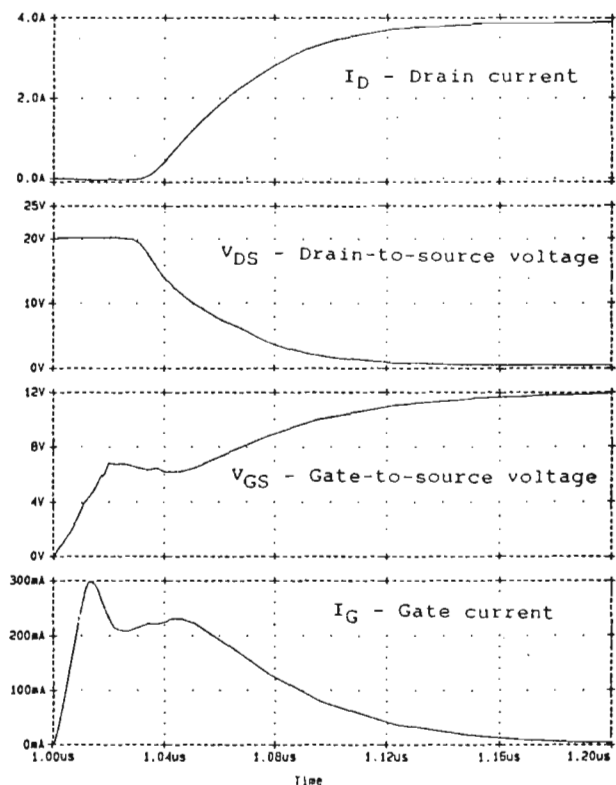
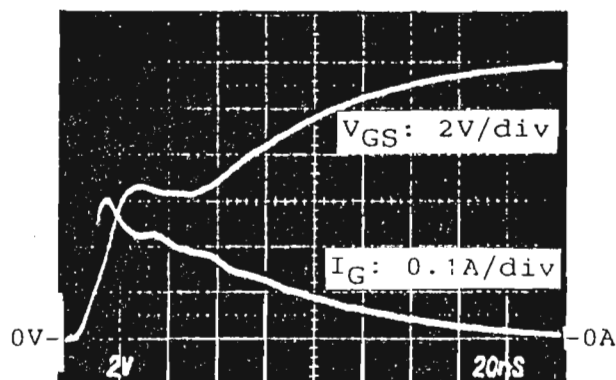
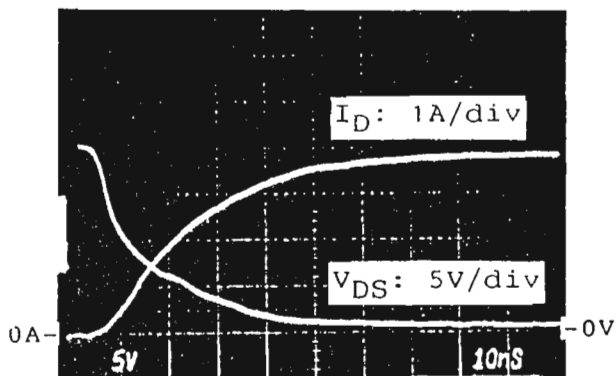


Figure 4a. Measured<sup>8</sup> and simulated Mosfet switching waveforms during turn-on in a resistive load circuit.

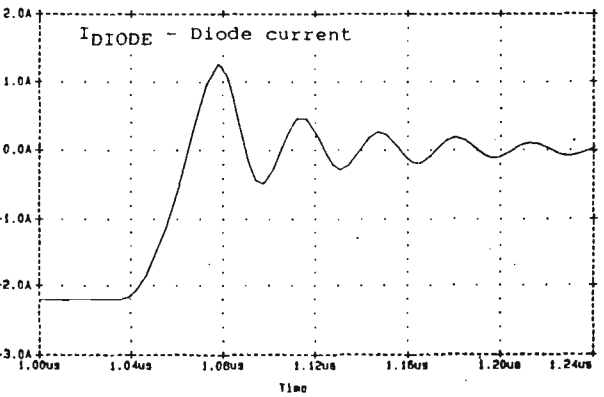
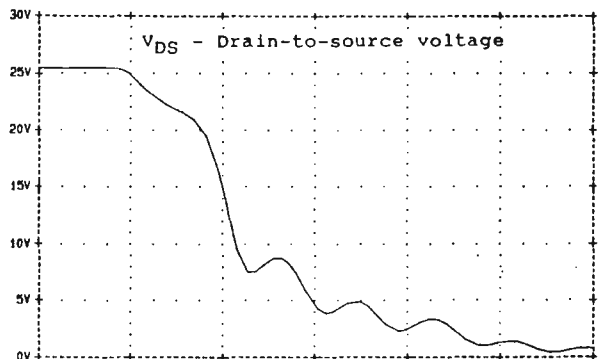
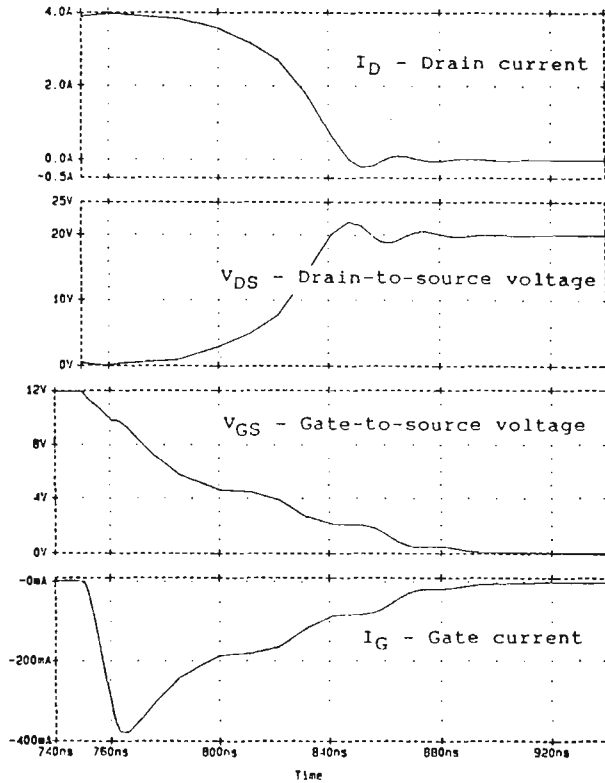
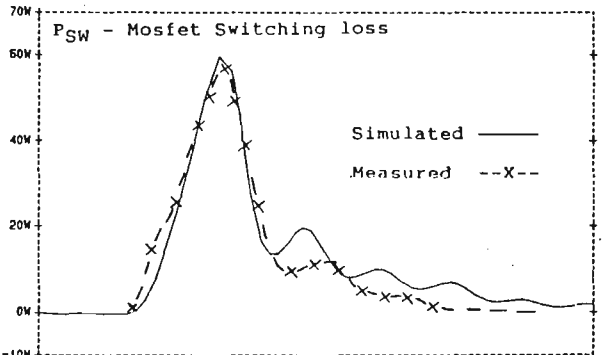
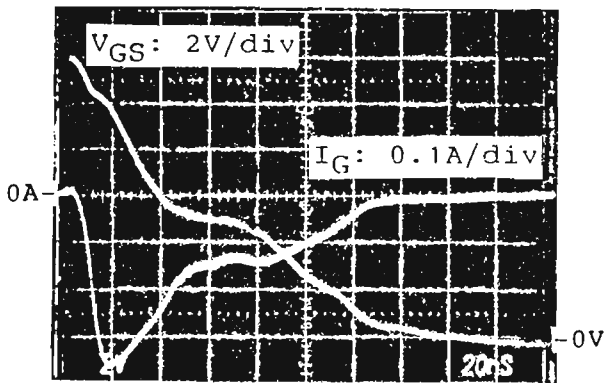
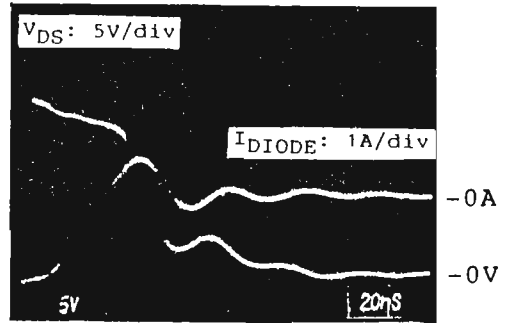
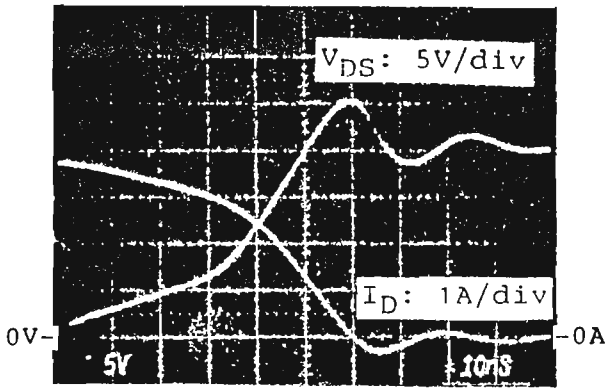


Figure 4b. Measured<sup>8</sup> and simulated Mosfet switching waveforms during turn-off in a resistive load circuit.

Figure 5. Measured<sup>12</sup> and simulated switching waveforms from a buck (step-down) switchmode converter during turn-on.

The switching performance of the Mosfet model was tested in a resistive load switching circuit. The test circuit has an IRF130 Mosfet switching a resistive load of 50ohm carrying a current of 4amp, with a 12V pulse generator connected to the gate, transition times of 11nsec, and an impedance of 25ohm and 80nhenry. Measured waveforms from the circuit are taken from Minasian<sup>8</sup>, and are shown with simulated waveforms in Figure 4. Very good agreement is shown between simulated and measured waveforms. Switching waveform transition parameters of particular interest from the simulation, such as 10% to 90% rise and fall times, correlate to within 8.2% (worst case) of the experimental data.

The performance of the Mosfet model was also tested in a 25V to 10V, 25W buck (step-down) type square-wave converter operating at 100kHz. Measured results from Minasian<sup>12</sup> are shown in Figure 5, along with simulated results. Results from Minasian do not detail parasitic component values, so estimated values are used in the simulation. Close agreement is achieved between measured and simulated waveforms, and the turn-on switching loss waveform demonstrates the practical application of simulation to the analysis of a switchmode circuit.

#### FLYBACK SWITCHMODE POWER SUPPLY SIMULATION

With suitable component models available, conventional analogue simulation software can be used to generate voltage and current waveforms occurring in a switchmode converter. A frequency spectrum of any periodic time-domain waveform in the circuit can be obtained by use of a Fast Fourier Transform (FFT) on the waveform. In this section a flyback switchmode converter is modelled and a frequency spectrum of the simulated conducted interference is compared with a measured response.

Initial modelling procedures for predicting conducted interference levels from switchmode supplies<sup>13,14</sup> use idealized voltage/current sources to represent the waveforms across the switching device. In this paper, results are obtained from accurately simulated circuit waveforms.

A model has been developed of a 30W multi-output flyback switchmode power supply comprising a main +5V, 3.5amp output, 240VAC input and operating at approximately 40kHz. The power supply model is shown in Figure 6, and has been simplified by deleting circuit components that have no cycle-by-cycle effect on the power supplies operation. An input voltage source of 340VDC is used to represent the AC input voltage during a small fraction of a 20msec (50Hz) AC period. A standard 50ohm line impedance stabilization network (LISN) is connected at the input of the power supply to take conducted interference measurements as specified by 4,5.

The power supply comprises an AC mains interference filter followed by a rectifier bridge, DC filter capacitor CC4, high-voltage switching transistor Q1, ferrite transformer K12, schottky output rectifiers D1 and D6, and feedback winding LP1. Fine control of the output voltage is obtained by varying R3 (an opto-coupler in the original circuit). Major parasitic leakage paths to ground are represented by capacitors CHS and CPS.

Circuit operating waveforms were measured with the power supply normally connected in the PABX console, with no LISN connected between the mains and console, and with no data cables connected to the console. Simulated operating waveforms were matched with the measurements by adjusting the load resistors R0UT and R60UT, and the output voltage control resistor R3. Measured and simulated waveforms of:

- 1) V(RSH) - voltage across the emitter shunt resistor of transistor Q1,
- 2) VC(Q1) - collector voltage of transistor Q1,
- 3) I(LS) - transformer output secondary current,

are shown in Figure 7 and good agreement is observed.

Conducted interference measurements were taken at the Research Laboratories as specified by 4,5 using a quasi peak detection mode over the frequency range

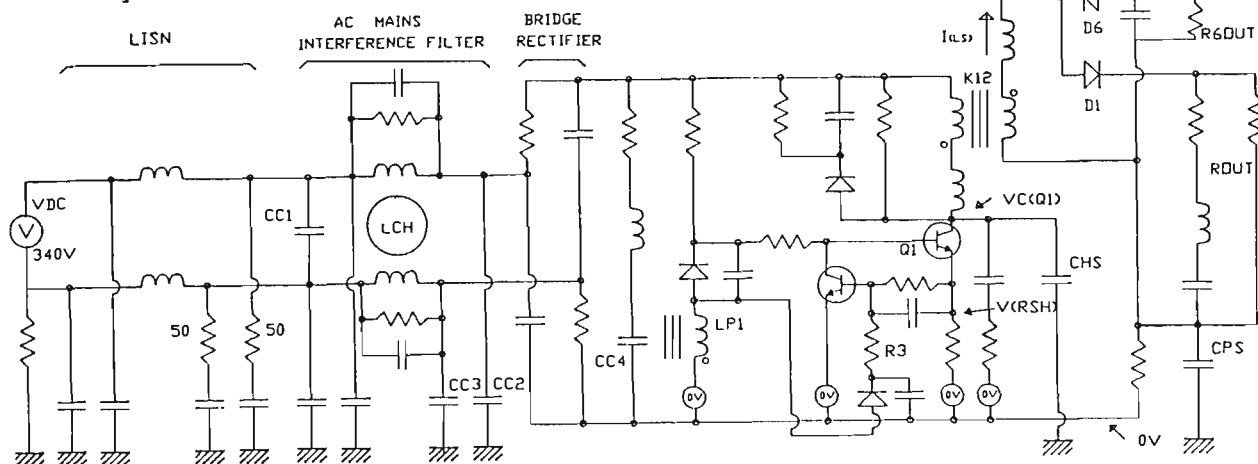


Figure 6. Simplified model of 30W flyback switchmode power supply and line impedance stabilisation network (LISN).

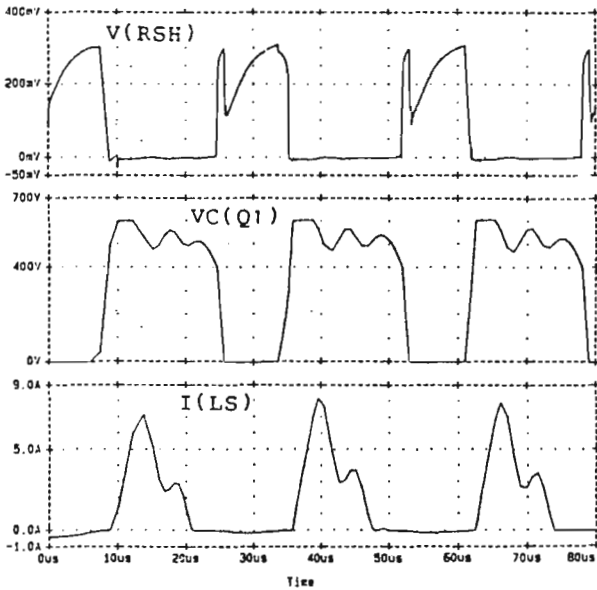
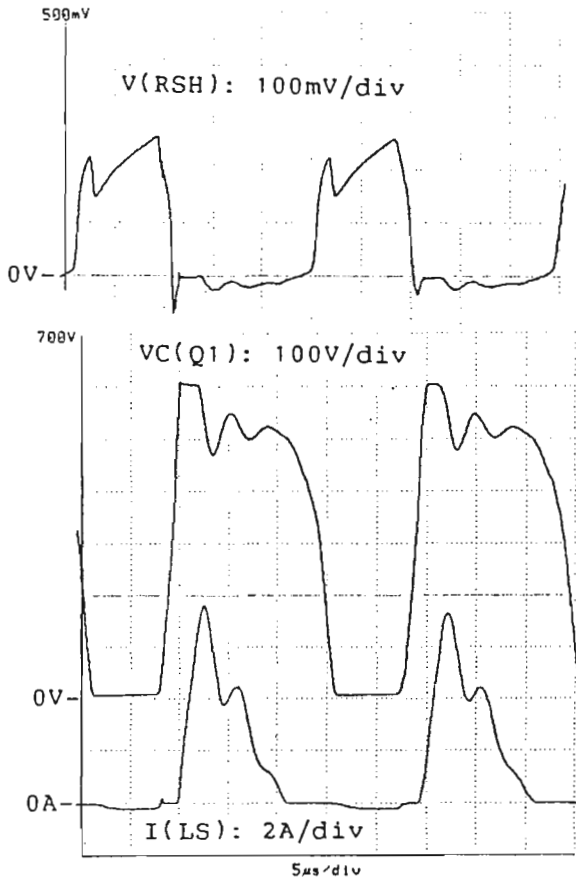


Figure 7. Measured and simulated waveforms from flyback switchmode power supply.

450kHz to 30MHz. However, accurately simulating the characteristics of the quasi peak detector mode has not yet been achieved.

At the Research Laboratories the retrofit solution to the interference problem focussed on reducing the common-mode (or antenna-mode) currents on the AC mains cord, as this was the main cause of customer complaint. A measurement using a current clamp was made of the absolute common-mode current on the console mains cord. The common-mode current is the vector sum of the active and neutral lead interference currents.

A simplified model of the LISN and converter indicating the interference current paths is shown in Figure 8. The power supply mains filter has been deleted for clarity. The LISN presents a low impedance path between the AC mains and the power supply at the power line frequency. At higher frequencies the LISN provides a 50 ohm impedance from each power supply line to ground, and a high impedance to the AC mains.

The common-mode currents  $I_1$  and  $I_2$  through the LISN are principally caused by high  $dV/dt$  across the capacitance to ground CHS of the switching transistor  $Q_1$ . The differential-mode current is principally caused by the voltage drop across the impedance of the DC filter capacitor  $CC_4$ .

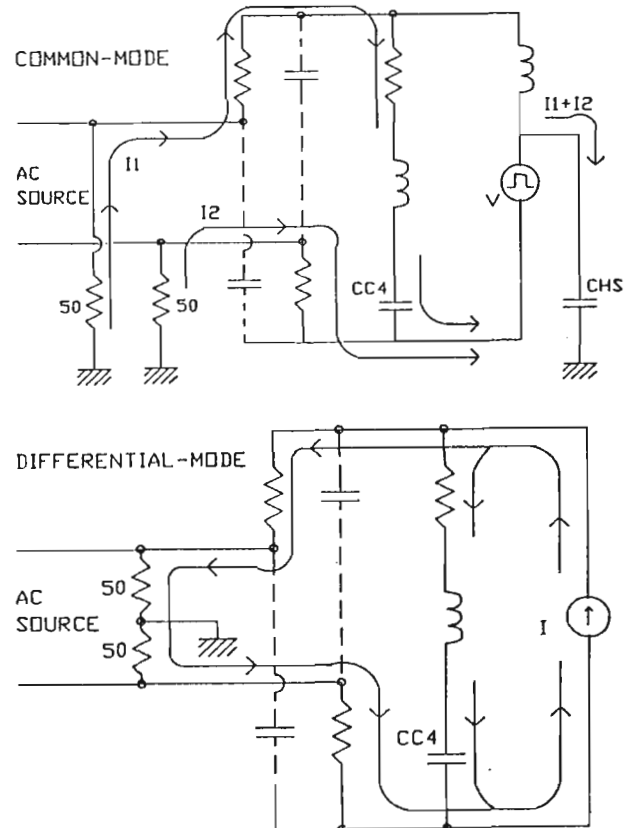


Figure 8. Simplified model of current paths in LISN and switchmode power supply for common-mode interference and differential-mode interference.

Common-mode currents are filtered by the mains filter capacitors CC2 and CC3 and the current compensated choke LCH, while differential mode current is filtered by the capacitor CC1 and the leakage inductance of the choke LCH.

The measured and simulated interference spectra of the common-mode current conducted from the power supply are shown in Figure 9. The simulated measurement is the sum of voltages in mV across the two 50 ohm LISN resistances, and is converted to dBuA to compare with the measured results.

The magnitude of interference is critically dependent on the parasitic capacitance values CHS and CPS. Typical capacitance values can be in the range 5pF to 100pF, and a value of 45pF is used for CHS and 100pF for CPS in this simulation, however neither value was measured. With these typical capacitance values, the simulated spectrum is in good agreement with the peaks of the measured spectrum in the measurement range 150kHz to 3MHz.

#### SUMMARY

Computer aided assessment of switchmode power supplies is fast becoming an option for the engineer. Significant advancements in processing speed and software application, coupled with suitable component models, has led to "brute force" simulation techniques being an accurate and time effective assessment tool. This paper has developed an accurate high-frequency power Mosfet model and has demonstrated the use of simulation techniques to predict switching loss and conducted interference in switchmode power supplies.

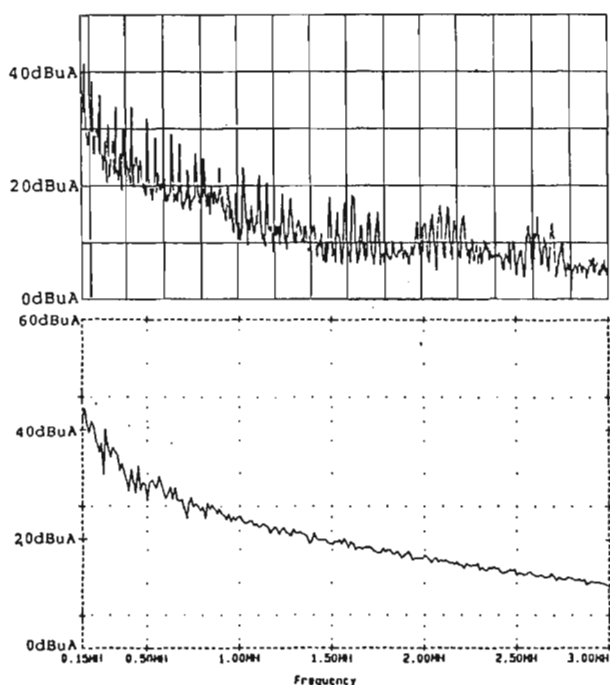


Figure 9. Measured and simulated interference spectra of conducted common-mode current from the flyback power supply.

#### ACKNOWLEDGEMENTS

The permission of the Executive General Manager, Research, of Telecom Australia to publish the above paper is hereby acknowledged.

#### REFERENCES

1. V. Bello, "Computer aided analysis of switching regulators using SPICE2", Power Electronics Specialists Conference 1980, pp.3-11.
2. M. Chi and C. Hu, "An intrinsic power Mosfet model for circuit design and analysis", Proc. of Powercon 10, 1983, h-2, pp.1-9.
3. J.C. Bowers and H.A. Nienhaus, "SPICE-2 computer models for HEXFETs", International Rectifier, Appl. Note 954A.
4. International Electrotechnical Commission (IEC), "Limits and methods of measurement of radio interference characteristics of information technology equipment", CISPR Publication 22, 1st Edition, 1985.
5. U.S. Code of Federal Regulations, Telecommunication, Title 47, Part 15, Subpart J, Computing Device, October 1, 1984.
6. K.H. Liu and F.C. Lee, "Zero-voltage switching technique in dc/dc converters," IEEE Power Electronics Specialists Conference, 1986.
7. R. Redl and N.O. Sokal, "High-frequency switching-mode power converters: general considerations, and design examples at 0.6, 1, and 14 MHz," High Frequency Power Conversion Conference, May 1986 Proc., pp.265-296.
8. R. A. Minasian, "Power Mosfet dynamic large-signal model", IEE Proc., Vol.130, Pt.1, No.2, April 1983, pp.73-79.
9. E.S. Oxner, "Analyzing and controlling the tendency for oscillation of parallel power Mosfets", Proc. of Powercon 10, 1983, G1-2, pp.1-5.
10. H.P. Yee and P.O. Lauritzen, "SPICE models for power Mosfets: an update," IEEE Applied Power Electronic Conference 1988, pp.281-289.
11. C.H. Xu and D. Schroder, "Modelling and simulation of power Mosfet's and power diodes," IEEE Power Electronics Specialists Conference, April 1988, pp.76-83.
12. R.A. Minasian, "Power Mosfet transistors in high frequency switched mode power converters," IRECON, 19th International Electronics Convention, Institution of Radio and Electronics Engineers Australia, Sept.1983, pp.634-636.
13. M.J. Nave, "Prediction of conducted emissions in switched mode power supplies," IEEE EMC Symp. 1986, pp.167-173.
14. T. Rogne and A. Steinbakk, "Computer aided analysis of a multi-winding flyback converter including the EMI line filter," INTELEC 1987, pp.472-479.